

Debris disc candidates in systems with transiting planets

A. V. Krivov^{*}, M. Reidemeister, S. Fiedler, T. Löhne, and R. Neuhäuser

Astrophysikalisches Institut, Friedrich-Schiller-Universität Jena, Schillergäßchen 2–3, 07745 Jena, Germany

Accepted 2011 August 15. Received 2011 August 11; in original form 2011 June 1

ABSTRACT

Debris discs are known to exist around many planet-host stars, but no debris dust has been found so far in systems with transiting planets. Using publicly available catalogues, we searched for infrared excesses in such systems. In the recently published Wide-Field Infrared Survey Explorer (*WISE*) catalogue, we found 52 stars with transiting planets. Two systems with one transiting “hot Jupiter” each, TrES-2 and XO-5, exhibit small excesses both at $12\ \mu\text{m}$ and $22\ \mu\text{m}$ at a $\gtrsim 3\sigma$ level. Provided that one or both of these detections are real, the frequency of warm excesses in systems with transiting planets of 2–4% is comparable to that around solar-type stars probed at similar wavelengths with *Spitzer’s* MIPS and IRS instruments. Modelling suggests that the observed excesses would stem from dust rings with radii of several AU. The inferred amount of dust is close to the maximum expected theoretically from a collisional cascade in asteroid belt analogues. If confirmed, the presence of debris discs in systems with transiting planets may put important constraints onto formation and migration scenarios of hot Jupiters.

Key words: planetary systems – planets and satellites: detection – circumstellar matter – stars: individual: XO-5, HAT-P-5, TrES-2 parent star, CoRoT-8

1 INTRODUCTION

Many debris discs have been found in systems with known radial velocity (RV) planets (e.g. Beichman et al. 2005a; Moro-Martín et al. 2007; Trilling et al. 2008; Bryden et al. 2009; Kóspál et al. 2009), and a few systems with debris discs and directly imaged planetary candidates are known (Kalas et al. 2008; Marois et al. 2008; Lagrange et al. 2010). However, debris dust has not been found yet in systems with planets detected by transits.

In this paper, we search for debris dust in systems with transiting planets, using publicly available catalogues of transiting planets and several infrared (IR) surveys. The motivation is obvious. A successful search would extend the list of known “full” planetary systems that harbour both planets and asteroid or Kuiper belt analogs. Furthermore, it is the transit technique that allows determination of many planetary parameters, such as masses, radii and densities, and can provide insights into properties of planetary atmospheres and interiors. Finally, transiting planets are on the average even closer to their parent stars than those discovered by the RV method, which might be related to somewhat different formation circumstances. Therefore, systems with transiting planets are of special interest. Detection of planetesimal belts, which are leftovers of planet formation, could help constraining various formation and evolution scenarios

of those planets. And conversely, precise knowledge of planetary parameters could put constraints on the properties of the planetesimal belts. For instance, accurate masses and orbits of planets would result in tighter constraints on dynamical stability zones and thus location of planetesimal belts.

2 SEARCH FOR DUST

A list of 93 currently known systems with transiting planets was taken from exoplanets.org (Wright et al. 2011)¹. This list was compared with target lists of several IR missions: *IRAS* (Neugebauer et al. 1984), *ISO* (Kessler et al. 1996), *Spitzer* (Werner et al. 2004), *AKARI* (Murakami et al. 2007), and *WISE* (Wright et al. 2010), which we accessed through IRSA, the NASA/IPAC Infrared Science Archive at <http://irsa.ipac.caltech.edu>.

2.1 *IRAS*, *ISO*, *Spitzer*, and *AKARI*

Nearly all of the transit planet host stars are located at hundreds of parsecs from the Sun and are thus faint. Accordingly, we had not expected to find them in older, and shallower, *IRAS* and *ISO* catalogues and indeed, have not found any. For example, of 93 systems with transiting planets listed

^{*} krivov@astro.uni-jena.de (AVK)

¹ Accessed on May 11, 2011.

in *exoplanets.org*, only five are within 50 pc. These are GJ 436, GJ 1214, HAT-P-11, HD 189733, and HD 209458. None of them appears in *IRAS*, *ISO*, and *WISE* catalogues. Three of them, GJ 436, HD 189733, and HD 209458, have been probed by *Spitzer*/MIPS at 24 and 70 μm , yielding no excess detection (Bryden et al. 2009). We found an entry for the latter star in the *AKARI* catalogue, reporting a detection at 9 μm , which is consistent with the photospheric level. Note that HD 209458b was the first exoplanet found to transit the disc of its parent star (Charbonneau et al. 2000).

We have also identified two more distant transit planet host stars that were observed by *Spitzer*/MIPS: HD 80606 and HD 149026. No excess at 24 and 70 μm was found for HD 189733 (Bryden et al. 2009). For HD 80606, the result is ambiguous due to pointing problems (Carpenter et al. 2008). *AKARI* has observed one more transit host star, too: HD 149026. It has been detected at 9 μm , showing no excess.

2.2 WISE

The search in the *WISE* Preliminary Source Catalog was more successful. This is perhaps not a surprise, given the broad sky coverage (57%) of the catalogue, an excellent sensitivity of the instrument and thus a huge number of sources observed (257 million). The *WISE* catalogue provides measured magnitudes in four bands W_i ($i = 1, \dots, 4$), which are centred at 3.4, 4.6, 12, and 22 μm . Of 93 systems with transiting planet candidates listed in *exoplanets.org*, we found 53 with entries in the *WISE* catalogue. One source — CoRoT-14 — is irretrievably contaminated by ghost images in bands W_3 and W_4 and was excluded from further analysis.

To select possible IR excess candidates amongst the remaining 52 sources, we first converted the observed magnitudes in the four bands into spectral flux densities. Since no excesses are expected in bands W_1 and W_2 , we made simple photospheric predictions for W_3 and W_4 from the W_1 and W_2 fluxes. At first, we roughly corrected the W_1 and W_2 fluxes for an expected average level of interstellar extinction. Considering that systems in our sample are typically at a few hundreds parsecs, we set A_V to 0.5^m, which translates to $A(W_1) = 0.029^m$ and $A(W_2) = 0.012^m$ (Rieke & Lebofsky 1985). We then fitted the corrected W_1 and W_2 fluxes with a power law $F_{\text{phot}} = F_{\text{phot}}^0 \lambda^{-b}$, with F_{phot}^0 and b being the fitting parameters. Subtracting the expected photospheric flux from the observed one, we derived the “excess flux” $F \equiv F_{\text{obs}} - F_{\text{phot}}$ in bands W_3 and W_4 . The net uncertainty of a photometric point for a given star in the band W_3 or W_4 was computed as $\sigma = \sqrt{\sigma_{\text{phot}}^2 + \sigma_{\text{obs}}^2 + \sigma_{\text{cal}}^2}$. Here, σ_{phot} is the photospheric uncertainty, which we estimated from the combined uncertainties of the measurements in bands W_1 and W_2 , given in the *WISE* catalogue. Next, σ_{obs} is the measurement uncertainty in the bands of interest, W_3 and W_4 , also taken from the *WISE* catalogue. Finally, σ_{cal} is the absolute calibration uncertainty of the *WISE* instrument (2.4, 2.8, 4.5, and 5.7% for bands from W_1 to W_4). The significance of an excess can now be defined as $\chi = F/\sigma$.

The distributions of χ -values in the sample are shown in Fig. 1 for bands W_3 (top) and W_4 (bottom). The W_3 histogram appears close to gaussian, without any obvious outliers. However, the W_4 histogram uncovers a bin containing four systems with $\chi > 1.75\sigma$, clearly separated from the gaussian bulk. These are XO-5, HAT-P-5, TrES-2, and

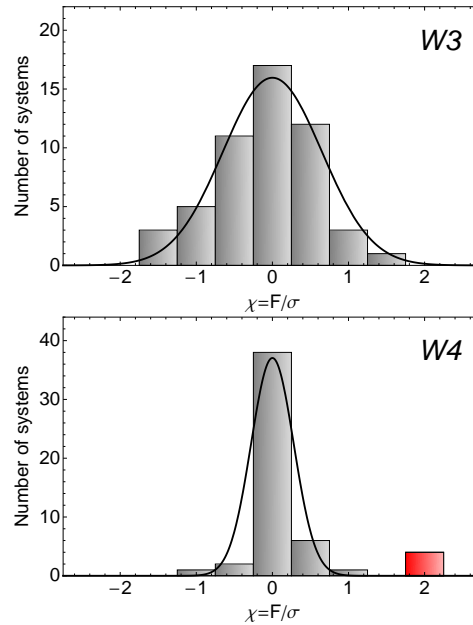


Figure 1. Histogram of $\chi = F/\sigma$ values at 12 μm (top) and 22 μm (bottom) for systems with transiting planets. For comparison, overplotted are closest gaussian distributions, which have variances of 0.65 (top) and 0.28 (bottom). That these variances are smaller than unity may suggest that the procedure of calculating σ , described in the text, is too cautious and overestimates the actual noise. The rightmost bin in the W_4 histogram shown in red contains four excess candidates. We checked that slight modifications to the photospheric extrapolation procedure or extinction correction (i.e. using A_V values between 0.0^m and 1.0^m) slightly skew and shift the W_3 histogram, but preserve the W_4 one, including the bin with the four outliers.

CoRoT-8. These four excess candidates will be checked in Sect. 3 more thoroughly, including an in-depth photospheric analysis and more accurate uncertainty estimates.

3 ANALYSIS OF EXCESS CANDIDATES

For the excess candidates, we have collected stellar data (Tab. 1) as well as optical and near-IR photometry. In the visual, we used the USNO-B1.0 Catalog (Monet et al. 2003), the Guide Star Catalog, Vers. 2.3.2 (Lasker et al. 2008), and the All-Sky Compiled Catalogue of 2.5 Million Stars (Kharchenko & Roeser 2009). The near-IR data stem from the 2MASS All-Sky Catalog of Point Sources (Skrutskie et al. 2006). For transforming the B , V , R , I magnitudes into units of flux density [Jy], we used the Johnson calibration system and for the 2MASS J , H , K_s bands the Cohen et al. (2003) calibrations.

At the first step, this photometry was corrected for interstellar extinction. Since for distances considered here the latter is known to correlate with distance only weakly, we used colour indices from Kenyon & Hartmann (1995) and the spectral type as given in Tab. 1 to derive the best-fit A_V from multiple colours and then A_λ/A_V ratios of Rieke & Lebofsky (1985) to compute extinction for the wavelengths of all photometry points. The derived A_V values are within 0.1^m for non-CoRoT stars, but as large as

Table 1. Stellar parameters.

Star	V_{mag}	d [pc]	SpT	M_{\star} [M_{\odot}]	T_{eff} [K]	R_{\star} [R_{\odot}]	Ref.	d [pc]	T_{eff} [K]
XO-5	12.1	260 ± 12	late G	0.88 ± 0.03	5370 ± 70	1.08 ± 0.04	[1]	$286 (+10\%)$	$5800 (+8\%)$
HAT-P-5	12.0	340 ± 30	early G	1.16 ± 0.06	5960 ± 100	1.17 ± 0.05	[2]	$340 (\pm 0\%)$	$6400 (+7\%)$
TrES-2	11.4	230	G0 V	1.08 ± 0.11	5960 ± 100	$1.00^{+0.06}_{-0.04}$	[3]	$219 (-5\%)$	$6400(+7\%)$
CoRoT-8	14.8	380 ± 30	K1 V	0.88 ± 0.04	5080 ± 80	0.77 ± 0.02	[4]	$304 (-20\%)$	$5400 (+6\%)$

References: [1] Pál et al. (2009), [2] Bakos et al. (2007), [3] O’Donovan et al. (2006), [4] Bordé et al. (2010).

Note: The last two columns list best-fit values and their deviation from the starting values.

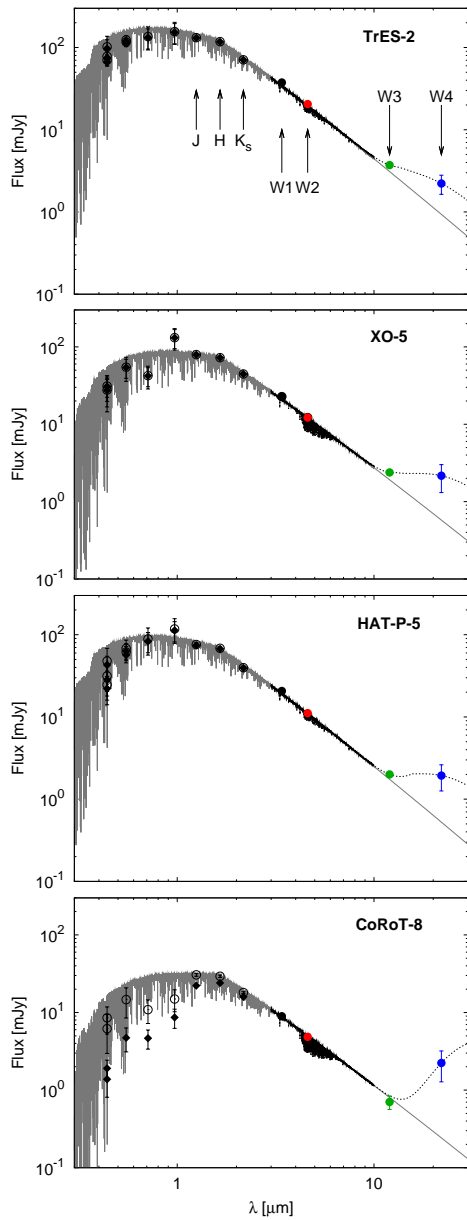


Figure 2. Spectral energy distributions (SEDs) of four selected stars. Grey solid line: predicted extinction-corrected photosphere. Diamonds and open circles: visual and near-IR photometry data before and after correction for interstellar extinction, respectively. Filled circles: extinction-corrected *WISE* data (errors bars are σ_{obs}). Black dashed line: modified BB model.

$1.3^m \pm 0.2^m$ for CoRoT-8. The extinction in W3 and W4 bands does not exceed 0.04^m (CoRoT-8).

At the second step, we performed a minimum χ^2 fitting of the extinction-corrected stellar photospheric fluxes by NextGen models (Hauschildt et al. 1999), only to data points between $1 \mu\text{m}$ and $5 \mu\text{m}$. This is because those wavelengths are short enough not to expect any excess emission, but are long enough for interstellar extinction to be small. The interval from $1 \mu\text{m}$ to $5 \mu\text{m}$ includes three 2MASS points (J , H , K_s) and two *WISE* points (3.4 and $4.6 \mu\text{m}$), all of which were given equal weights. Since the surface gravity of our stars ($\log g$ between 4.33 and 4.61) and their metallicity ($[\text{Fe}/\text{H}]$ from -0.2 to $+0.31$) deviate from the solar values only slightly (see Tab. 1 for references), we assumed a $\log g$ of 4.5 and the solar metallicity. Using T_{eff} and d listed in Tab. 1 as starting values, we varied the temperature by ± 400 K in 200 K steps and the distance to the star within $\pm 30\%$ in 5% steps to derive best-fit values of these two parameters. This yielded deviations from the starting values of up to 8% in T_{eff} and up to 20% in d (Tab. 1). The results with the photometric points overplotted are shown in Fig. 2. Importantly, TrES-2 and XO-5 and possibly also HAT-P-5 reveal small excesses in band W3 as well, which were not seen in Fig. 1 (top).

We now come to a detailed analysis of the fluxes and their uncertainties. Denote the observed flux by F_{obs}^* , the extinction-corrected one by F_{obs} , the predicted extinction-corrected photospheric flux by F_{phot} , and the excess flux by $F \equiv F_{\text{obs}} - F_{\text{phot}}$. As in Sect. 2, the net uncertainty of F for a given star in band W_3 or W_4 is computed as $\sigma = \sqrt{\sigma_{\text{phot}}^2 + \sigma_{\text{obs}}^2 + \sigma_{\text{cal}}^2}$. The measurement uncertainty σ_{obs} and the calibration uncertainty σ_{cal} are included as described before. However, the photospheric uncertainty σ_{phot} is now a by-product of the fitting procedure. It is dominated by a scatter in J , H , K_s , W_1 , and W_2 points (the error bars of the points themselves as well as the uncertainty of the extinction correction are much smaller). All the quantities above, and the resulting excess significance $\chi = F/\sigma$, are listed in Tab. 2. Nearly all excesses are at $\approx 2\sigma$ level, whereas usually a 3σ excess is treated as a significant detection. However, in the cases of TrES-2, XO-5, and HAT-P-5, the excess is detected in two bands. The combined multi-band (W_3 and W_4) gaussian statistics suggests the significance level for these sources of 3.28, 3.23, and 2.82, respectively. This finally selects two systems, TrES-2 and XO-5, as $> 3\sigma$ -significant and thus the best excess candidates. The binomial probability that one of these two detections is false is only 6.4%, and the probability that both are false is as low as 0.2%. The expected number of false detections at $> 3\sigma$ level is just 0.14; we detected two excesses at that level.

Table 2. Fluxes [mJy], uncertainties [mJy], and significance of excesses.

System	Band	F_{obs}^*	F_{obs}	F_{phot}	F	σ_{phot}	σ_{obs}	σ_{cal}	σ	χ	χ_{joint}
TrES-2	W3	3.71	3.72	3.10	0.62	0.20	0.11	0.17	0.29	2.17	3.28
	W4	2.22	2.22	0.93	1.29	0.12	0.58	0.13	0.61	2.12	
XO-5	W3	2.38	2.38	1.92	0.47	0.09	0.14	0.11	0.20	2.35	3.23
	W4	2.16	2.16	0.58	1.58	0.08	0.85	0.12	0.86	1.84	
HAT-P-5	W3	1.99	2.00	1.74	0.26	0.09	0.10	0.09	0.16	1.58	2.82
	W4	1.93	1.94	0.53	1.41	0.09	0.68	0.11	0.70	2.03	
CoRoT-8	W4	2.17	2.24	0.24	2.00	0.09	0.96	0.13	0.97	2.05	

Columns: Observed flux F_{obs}^* , observed flux after correction for extinction F_{obs} , expected photospheric flux F_{phot} , excess flux F ; uncertainty of photospheric flux σ_{phot} , observation uncertainty σ_{obs} , absolute calibration uncertainty σ_{cal} , net uncertainty of the excess flux σ , excess significance level in a single band χ ; joint (W_3 and W_4) significance level χ_{joint} .

Table 3. Dust parameters inferred from the observed excesses and parameters of transiting planets.

System	Blackbody		Modified blackbody						Planet		
	T_{d} [K]	r_{d} [AU]	s_{blow} [μm]	s_0 [μm]	T_{d} [K]	r_{d} [AU]	M_{d} [M_{\oplus}]	f_{d}	a_{pl} [AU]	e_{pl}	M_{pl} [M_{jup}]
TrES-2	218	1.7	0.4	2.1	155	5.8	5×10^{-5}	3×10^{-4}	0.037	0 (fixed)	1.28
XO-5	181	2.2	0.4	2.0	133	8.0	1×10^{-4}	6×10^{-4}	0.051	0.049	1.06

Note: Planetary parameters are taken from the papers listed in Tab. 1.

4 PRESUMED DUST BELTS

In what follows, we estimate the parameters of dust that would produce the excesses in the best candidate systems, TrES-2 and XO-5, provided these are real. Since the excesses are of low significance and the data are limited to two photometry points, a detailed SED modelling based on various assumptions about the size distribution and composition of dust is not warranted. Instead, we used a pure blackbody (BB) and a modified BB emission model. In the latter case, we assumed a single grain size s_0 and the opacity index of -2 beyond $\lambda = 2\pi s_0$. The effective grain size s_0 was chosen in the following way. Assuming a power-law size distribution with the index $q = 3.5$ and the lower cutoff radius s_{min} of twice the radiation pressure blowout limit s_{blow} (see. e.g., Krivov et al. 2006; Thébaud & Augereau 2007), we have equated the emission of a disc of grains having such a size distribution and the emission of a disc composed of equal-sized grains of radius s_0 :

$$\int_{s_{\text{min}}}^{\infty} Q_{\text{abs}}(\lambda, s) B_{\nu}(\lambda, T_{\text{d}}(r_{\text{d}}, s)) s^{2-q} ds = Q_{\text{abs}}(\lambda, s_0) B_{\nu}(\lambda, T_{\text{d}}(r_{\text{d}}, s_0)) s_0^2 \int_{s_{\text{min}}}^{\infty} s^{-q} ds, \quad (1)$$

where r_{d} is the distance from the star, λ is the wavelength where excess emission is observed, B_{ν} is the Planck intensity, $Q_{\text{abs}}(\lambda, s)$ is the grain absorption efficiency, and T_{d} is the grain temperature. In calculating s_{blow} , we assumed the unit radiation pressure efficiency and the bulk density of 3 g cm^{-3} and took the stellar parameters from Tab. 1. Equation (1) was solved for s_0 .

We then sought pure BB and modified BB curves that reproduce $F(12 \mu\text{m})$ and $F(22 \mu\text{m})$. This has yielded estimates of the temperature, location, mass, and the fractional luminosity of the emitting dust (Tab. 3). When deriving the dust mass, we converted the mass of grains with $s = s_0$

into the mass of grains with $s < 1 \text{ mm}$, assuming a power-law size distribution with a slope of 3.5. Both stars, TrES-2 and XO-5, appear to have rings with radii of 6–8 AU and fractional luminosities in the range $(3\text{--}6) \times 10^{-4}$. We stress that all these inferred values are quite uncertain, because they rest on scarce photometric data and their derivation involves a number of simplifying assumptions and poorly known parameters.

5 CONCLUSIONS AND DISCUSSION

We have found that two out of 52 systems with transiting planets observed by *WISE* reveal warm two-band (12 and $22 \mu\text{m}$) IR excesses at $> 3\sigma$ level. The probability that both excesses are real is 94% and that one of them is real is 99.8%.

Provided that one of the two systems, or both, do possess a warm disc, this would imply the excess incidence rate of 2–4%. For comparison, the *Spitzer*/MIPS detection rate of $24 \mu\text{m}$ excesses around old ($\sim 4 \text{ Gyr}$) field stars was found to be 1/69 ($1 \pm 3\%$) (Bryden et al. 2006). Another sample of solar-type stars probed by MIPS at $24 \mu\text{m}$ resulted in $\approx 4\%$ detection rate, averaged over all ages (Trilling et al. 2008). Lawler et al. (2009) analyzed *Spitzer*/IRS observations of nearby solar-type stars and found excess around 12% of them in the long-wavelength IRS band ($30\text{--}34 \mu\text{m}$), but only 1% of the stars have detectable excess in the short wavelength band ($8.5\text{--}12 \mu\text{m}$). Thus the frequency of warm excesses around solar-type stars with transiting planets seen in the *WISE* data may be comparable to that in unbiased samples of similar stars found with *Spitzer*.

Each of the two systems discussed here hosts one known close-in planet and, if the excesses are real, an asteroid belt-size dust ring well outside the planetary orbit. In both cases, more planets could orbit both inside and outside the belts. Additional planets at $\lesssim 10 \text{ AU}$ could be revealed by in-depth

RV analyses, by transits, or by transit time variations of already known planets (Maciejewski et al. 2011a). The latter method was used for TrES-2 (Rätz et al. 2009) and XO-5 (Maciejewski et al. 2011b). Non-detection is consistent with the presence of debris belts at several AU, which are incompatible with planets in that region. In the case of TrES-2, Rätz et al. (2009) noticed a second dip in the light curve, both in their own light curves and those published in the literature. This second dip has been observed several times and then disappeared. In addition to other possible reasons for this effect, discussed by Rätz et al., it could be due to an occultation by material in the debris disc. Estimates show that a clump of dust produced in a recent collision of two ~ 100 km-sized planetesimals would bear enough cross section to account for such a dip before it is azimuthally spread into a ring in a few years, although the probability of witnessing such an event is low.

Planets at largest orbital radii ($\gtrsim 10$ AU) will be hard to find by the transit technique. Direct imaging and astrometry are not feasible either, since these systems are too old and too distant. It will also be difficult to search for possible Kuiper belt analogues on the periphery of the systems, because they are too faint for far-IR facilities such as *Herschel*. However, future mid-IR instruments such as *JWST/MIRI* should have enough sensitivity to study warm dust in great detail, including dust grain spectroscopy. They may also take a closer look at further potential excess candidates such as HAT-P-5 and CoRoT-8 identified in this study.

The origin and the production mechanisms of the presumed dust are unclear. We have computed the dust mass expected to be produced through a steady-state collisional cascade in a belt of “asteroids” with moderate eccentricities, using the model of Löhne et al. (2008) with a velocity-dependent critical fragmentation energy from Stewart & Leinhardt (2009). At ages of ~ 1 Gyr, the maximum expected dust mass is $\sim 10^{-4} M_{\oplus}$ at $r_d = 10$ AU and $\sim 10^{-5} M_{\oplus}$ at $r_d = 6$ AU. Comparing with Tab. 3, we conclude that the amount of dust in our systems is close to, or even somewhat greater than, the theoretical maximum allowed by a steady-state collisional cascade. This means that we might have a similar difficulty that exists in explaining other systems with hot excesses that have been known before, such as HD 69830 (Beichman et al. 2005b). Proposed scenarios for such systems include: supply of comets from an outer massive cometary reservoir, possibly following a recent dynamical instability such as the Late Heavy Bombardment; the inward-scattering and desintegration of a large object from such an outer reservoir; a recent major collision between two large planetesimals (see Payne et al. 2009, and references therein). Finally, a possibility of a steady-state collisional dust production can be resuscitated if one allows the asteroids in the belt to have very eccentric orbits (Wyatt et al. 2010). Such a belt could result from shepherding and scattering of an initial planetesimal belt during the inward migration of “hot Jupiters” (Payne et al. 2009).

ACKNOWLEDGMENTS

We are most grateful to the anonymous reviewer for valuable and constructive comments that helped to improve the manuscript significantly. Our thanks go to Ronny Errmann

for his assistance in calculating the interstellar extinction. This research has made use of the Exoplanet Orbit Database and the Exoplanet Data Explorer at exoplanets.org. Our work was funded by the German DFG, grants Kr 2164/9-1 and Lo 1715/1-1. SF acknowledges support of the State of Thuringia via the graduate student fellowship.

REFERENCES

- Bakos G. Á. et al., 2007, *ApJL*, 671, L173
 Beichman C. A. et al., 2005a, *ApJ*, 622, 1160
 Beichman C. A. et al., 2005b, *ApJ*, 626, 1061
 Bordé P. et al., 2010, *A&A*, 520, A66
 Bryden G., et al., 2009, *ApJ*, 705, 1226
 Bryden G. et al., 2006, *ApJ*, 636, 1098
 Carpenter J. M. et al., 2008, *ApJS*, 179, 423
 Charbonneau D., Brown T. M., Latham D. W., Mayor M., 2000, *ApJL*, 529, L45
 Cohen M., Wheaton W. A., Megeath S. T., 2003, *AJ*, 126, 1090
 Hauschildt P., Allard F., Baron E., 1999, *ApJ*, 512, 377
 Kalas P. et al., 2008, *Sci*, 322, 1345
 Kenyon S. J., Hartmann L., 1995, *ApJS*, 101, 117
 Kessler M. F. et al., 1996, *A&A*, 315, L27
 Kharchenko N. V., Roeser S., 2009, ‘All-sky Compiled Catalogue of 2.5 million stars’, *VizieR Online Data Catalog*.
 Kóspál Á., Ardila D. R., Moór A., Ábrahám P., 2009, *ApJL*, 700, L73
 Krivov A. V., Löhne T., Sremčević M., 2006, *A&A*, 455, 509
 Lagrange A. et al., 2010, *Sci*, 329, 57
 Lasker B. M. et al., 2008, *AJ*, 136, 735
 Lawler S. M. et al., 2009, *ApJ*, 705, 89
 Löhne T., Krivov A. V., Rodmann J., 2008, *ApJ*, 673, 1123
 Maciejewski G. et al., 2011a, *MNRAS*, 411, 1204
 Maciejewski G., Seeliger M., Adam C., Rätz S., Neuhäuser R., 2011b, *AcA*, 61, 25
 Marois C., Macintosh B., Barman T., Zuckerman B., Song I., Patience J., Lafrenière D., Doyon R., 2008, *Sci*, 322, 1348
 Monet D. G. et al., 2003, *AJ*, 125, 984
 Moro-Martín A. et al., 2007, *ApJ*, 658, 1312
 Murakami H. et al., 2007, *PASJ*, 59, 369
 Neugebauer G. et al., 1984, *ApJL*, 278, L1
 O’Donovan F. T. et al., 2006, *ApJL*, 651, L61
 Pál A. et al., 2009, *ApJ*, 700, 783
 Payne M. J., Ford E. B., Wyatt M. C., Booth M., 2009, *MNRAS*, 393, 1219
 Plavchan P., Jura M., Lipsky S. J., 2005, *ApJ*, 631, 1161
 Rätz S. et al., 2009, *AN*, 330, 459
 Rieke G. H., Lebofsky M. J., 1985, *ApJ*, 288, 618
 Skrutskie M. F. et al., 2006, *AJ*, 131, 1163
 Stewart S. T., Leinhardt Z. M., 2009, *ApJL*, 691, L133
 Thébault P., Augereau J.-C., 2007, *A&A*, 472, 169
 Trilling D. E. et al., 2008, *ApJ*, 674, 1086
 Werner M. W. et al., 2004, *ApJS*, 154, 1
 Wright E. L. et al., 2010, *AJ*, 140, 1868
 Wright J. T. et al., 2011, *PASP*, 123, 412
 Wyatt M. C., Booth M., Payne M. J., Churcher L. J., 2010, *MNRAS*, 402, 657